Pergamon

Journal of Atmospheric and Terrestrial Physics, Vol. 58, No. 10, pp. 1171–1187, 1996
Published by Elsevier Science Ltd
Printed in Great Britain.
0021-9169/96 $15.00 + 0.00

0021-9169(95)00103-4

Geomagnetic storms, the Dst ring-current myth and lognormal distributions

Wallace H. Campbell

U.S. Geological Survey, Mail Stop 968, Box 25046, Denver, CO 80225, U.S.A.

(*Received* 22 *March* 1995; *accepted in revised form* 24 *March* 1995)

Abstract—The definition of geomagnetic storms dates back to the turn of the century when researchers recognized the unique shape of the H-component field change upon averaging storms recorded at low latitude observatories. A generally accepted modeling of the storm field sources as a magnetospheric ring current was settled about 30 years ago at the start of space exploration and the discovery of the Van Allen belt of particles encircling the Earth. The Dst global 'ring-current' index of geomagnetic disturbances, formulated in that period, is still taken to be the definitive representation for geomagnetic storms. Dst indices, or data from many world observatories processed in a fashion paralleling the index, are used widely by researchers relying on the assumption of such a magnetospheric current-ring depiction. Recent in situ measurements by satellites passing through the ring-current region and computations with disturbed magnetosphere models show that the Dst storm is not solely a main-phase to decay-phase, growth to disintegration, of a massive current encircling the Earth. Although a ring current certainly exists during a storm, there are many other field contributions at the middle-and low-latitude observatories that are summed to show the 'storm' characteristic behavior in Dst at these observatories. One characteristic of the storm field form at middle and low latitudes is that Dst exhibits a lognormal distribution shape when plotted as the hourly value amplitude in each time range. Such distributions, common in nature, arise when there are many contributors to a measurement or when the measurement is a result of a connected series of statistical processes. The amplitude-time displays of Dst are thought to occur because the many time-series processes that are added to form Dst all have their own characteristic distribution in time. By transforming the Dst time display into the equivalent normal distribution, it is shown that a storm recovery can be predicted with remarkable accuracy from measurements made during the Dst growth phase. In the lognormal formulation, the mean, standard deviation and field count within standard deviation limits become definitive Dst storm parameters. Published by Elsevier Science Ltd

1. INTRODUCTION

Carefully studying the field changes in Bombay, Nanabhoy Moos (1919) the original director of the Indian Institute of Geomagnetism, discovered the existence of a unique pattern in geomagnetic disturbance. After removing the expected quiet-day field (Sq) levels, he averaged a number of the H-component disturbances, arranged in time corresponding to the start of the disturbance period, and discovered the 'classic' geomagnetic storm field: the positive H onset of disturbance followed by a rapid depression of H and then a slow recovery to the quiet level. Schmidt (1917) was the first to suggest that the storm-field decrease was due to a ring of westward electric current circling the Earth. The geomagnetic storm pattern was further explored by Chapman (1919, 1927, 1935) who used the name 'Dst' for this average storm-time (st) presentation of field disturbances (D) with regular daily variations and baseline main field levels removed. Chapman (1951) introduced the now familiar terms 'sudden commencement', 'initial phase', 'main phase' and 'recovery phase' to describe typical Dst storm characteristics. Scientists continue to accept to this day the Chapman and Ferraro (1931, 1932) explanation of the initial phase, positive field excursion of Dst as due to a compressional arrival of solar wind at the magnetospheric boundary. The focus of the present review is the stormtime variation that follows the initial phase.

Scientific interest in space grew rapidly following the start of the International Geophysical Year (IGY) of 1957–1958 and the 1964–1965 year of the quiet Sun (IQSY). During this period, Singer (1957) proposed a physical picture of a process that could generate a magnetospheric ring current for a geomagnetic storm; some scientists consider this paper to be the predictor of the spectacular Van Allen (1959, 1969) discovery of the Earth's charged particle belt. Akasofu and Chapman (1961) and Akasofu *et al.* (1961) calculated the ring-current properties from Dst characteristics.

Their depiction of the storm as a compressional onset followed by a rapid loading and subsequent unloading of a westward-flowing, current-ring of particles about the Earth became fixed in the minds of most space scientists at this time. In such an environment, only the axially aligned field component, $H/\cos\theta$ (where H is the horizontal field component and θ is the geomagnetic dipole latitude), need be monitored and averaged from a few low-latitude locations to represent the worldwide effects. Dst was assumed to fill the role exactly.

Sugiura (1961) studied the differences in Northern and Southern hemisphere solstitial-month Dst and found a significant seasonal effect. Akasofu and Chapman (1964) introduced the idea of a partial (local-time component) ring-current effect in Dst to justify the longitudinal differences of disturbances found at middle and low-latitude observatories. Hoffman and Bracken (1967) used estimates of average particle distributions from satellite observations (e.g. Frank, 1967) to produce a model of the westward and eastward ring currents that soon became the storm source-current picture favored by many researchers.

The first use of Dst as an index can be attributed to Vestine *et al.* (1947) who generalized the storm-time averaging procedure to include all UT hours and a global distribution of stations to represent the Earth's field variations during the Second Polar Year (1932–1933). Accepting a ring-current model of storms, Kertz (1964) devised a new method of Dst evaluation using only station night-time field values when the Sq quiet dynamo currents were essentially absent. Sugiura (1964) standardized the Dst procedure using eight, well-distributed, low-latitude observatories. This Dst preparation scheme was subsequently followed for the representation for the IGY-IQSY period. In 1969 at its Madrid assembly, the International Association of Geomagnetism and Aeronomy (IAGA) officially adopted the Sugiura form of Dst as a standard activity index.

The basic idea for the Dst is that the global part of a geomagnetic disturbance is what remains after local variation features and baseline values are removed from low-latitude station records. Differences in the values about the Earth are accommodated by averaging a number of observatories. With the assumption of an axially symmetric ring-current source, the use of only the H component of field and adjustment for the average station geomagnetic latitude become reasonable procedures. Figure 1 shows common scale H-component magnetograms for the present contributing observatories and the derived Dst index for the occasion of a typical geomagnetic storm of 19 December 1980.

Not all Dst storms show the 'classic' initial phase, main phase, recovery phase shapes. Some occasions obviously represent disturbance periods in which more than one storm has occurred and separated commencements, and/or peaks of the main phases can be recognized. On rare occasions, probably less than 1% of the large disturbance periods, the Dst index values do not follow the smooth growth and gradual decay form but rather seem more impulsive. Figure 2 of the 599 gamma Dst storm on 13 March 1989 shows an example. This storm was accompanied by major Polar Cap Absorption events, extensive proton precipitation and the unusual red auroras. The auroral zone was displaced to mid-latitudes; there were simultaneous electric power-line outages (from current induction) throughout the province of Quebec, Canada, and northeastern U.S.A. implying that the maximum field effects were centered near those locations (Allen *et al.*, 1989). The Dst observatory recordings at San Juan, Puerto Rico, were overwhelmed, apparently by the relatively nearby field-aligned and ionospheric current effects. Storms of this type are not the subject of this paper.

To describe periods of geomagnetic storms, most researchers use the term 'Dst' to indicate a global processing and averaging of all H-component, geomagnetic storm variations in a fashion similar to that of the index. In the present view of many scientists, the geomagnetic storm (Dst) main and recovery phases are unequivocal evidence of a magnetospheric ring current at about 4–8 Earth radii (Re) distance that grows rapidly and then slowly decays. Various applications of the index, e.g. for field adjustments in regional or global mapping, or as a source current for deep-Earth induction measurements, rely on this ring-current model for justification. Mayaud (1980), in his 'definitive' textbook on geomagnetic indices stated, "Among all geomagnetic indices, the Dst index is probably the one that monitors and records with greatest accuracy the phenomenon for which it was designed. This is due to the great simplicity of the magnetic variations caused by the ring current: they are very nearly axially symmetric and do not depend on longitude or local time." As we shall see, Mayaud's statement has become a Dst ring-current myth that is an incorrect representation of reality.

2. PROBLEMS WITH DST AS A RING-CURRENT REPRESENTATION

For quite a while, isolated studies showed some difficulties in the derivation of Dst as a full ring-current representation. Akasofu *et al.* (1963) could not

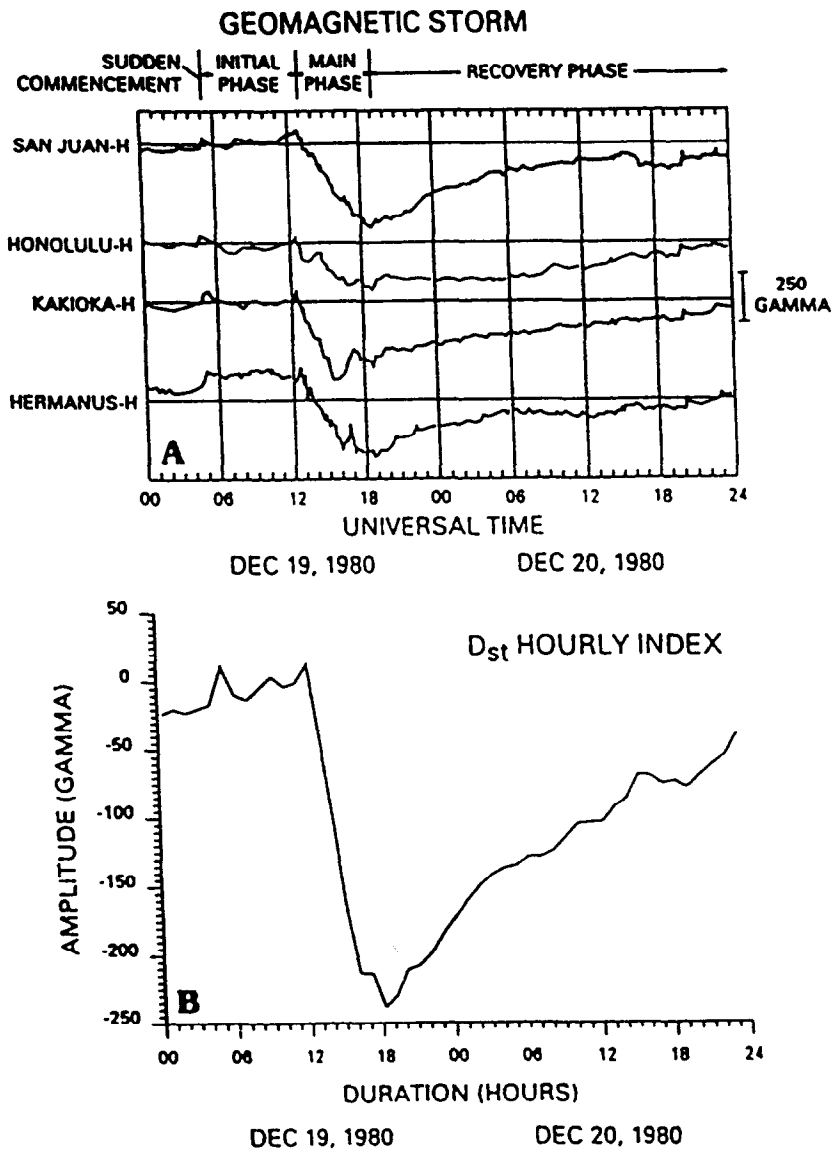

Fig. 1. The *H*-component field variations at Dst observatories (A) and the computed Dst hourly index (B) for a storm of 19 December 1980. Values supplied by the World Data Center A, Boulder, Colorado, U.S.A.

discover a single time constant to represent the recovery phase. Tarpley (1973) found that small changes in the quiet-day current (Sq) focus positions (near the Dst observatories) could cause major changes in the phase and amplitude of the Sq fields that are assumed to be simply removed from Dst. Matsushita *et al.* (1973) uncovered sector (IMF by field) effects in the Sq that are not accommodated in the Sq-field removal from Dst. Annual and semi-annual changes in the apparent main field levels at night (Campbell, 1984) were found to track the seasonal magnetotail positions. Effects of frequency dependent induction (Campbell and Schiffmacher, 1988) had not been accommodated by the standard index derivation. Carefully analyzing the Dst values, Stening (1990) identified the appearance of imbedded lunar tidal variations of ionospheric origin.

Stern (1991) gave an excellent review of the early substorm research, noting that "Chapman believed that magnetic storms were the fundamental feature while substorms were just an associated detail; in contrast, substorms are nowadays viewed as fundamental

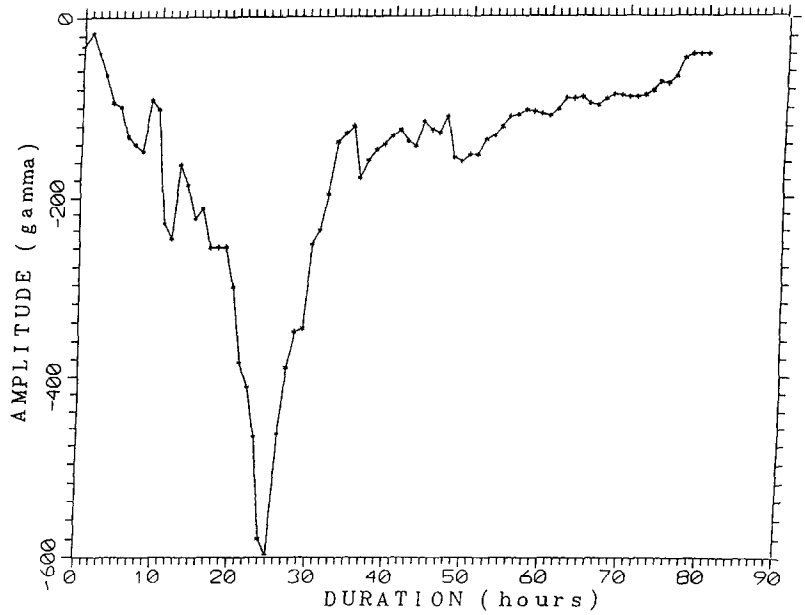

Fig. 2. Dst values for the extremely large storm of 13 March 1989 that caused electric power failures in eastern Canada and northeastern U.S.A. (Allen *et al.*, 1989). Values obtained from World Data Center A, Boulder, Colorado, U.S.A. This storm was an unusual 'polar cap blackout' type, rich in the precipitation that generates red-glow auroras.

and are studied in great detail, with relatively little attention given to magnetic storms." Part of the reason for this emphasis change is that the geomagnetic storm form evidenced by Dst has not been recoverable from the magnetospheric disturbance measurements. At best, it has only been possible to show that clusters of substorm activity correspond to the general period of depression of the Dst index (Akasofu and Chapman, 1972, figure 8.24 and pp. 602–604). In a review of the storm studies, Kamide (1979) indicated that there was no satisfactory way to determine the partition of energy between that observed directly in the polar ionosphere and that indicated by the storm ring-current of Dst.

Fundamental problems with the symmetric-ring model have been reported. Akasofu and Chapman (1964) found the storm fields to be asymmetric about the Earth. Subsequently, to accommodate this observation, combination models needed to be assumed with full and partial ring currents coexisting (e.g. Fukushima and Kamide, 1973). Early computations by Cummings (1966) showed that there should be strong field-aligned currents contributing to the low-latitude observations. The use of the cos Θ adjustment in Dst derivations (demanded by a ring model) was shown to be in error at night when the H and Z fields were found to triangulate to a magnetospheric position that varied during the storm progress and shifted with season in a regular fashion (Campbell, 1973).

Although satellite passes through the region of 3–9 R_e certainly show in situ evidence of the ring current existence, Lui *et al.* (1987) found that the storm-period values in the westward ring-current region had major temporal and spatial fine structures. There was not one simple global ring current, or a simple superposed partial ring current that gradually increased with the growing main phase of the Dst storm, and then slowly decreased with the decaying recovery phase of the Dst storm. Rather, there were many large and small partial ring currents varying greatly in time and location; radial as well as azimuthal currents exist on a variety of scales. The processes in that region cannot be modeled from the Dst; something other than a ring current must be responsible for defining the disturbance storm-time Dst shape. When considering the surface fields resulting from the currents, it is important to realize that the Earth's electrical conductivity is rising so rapidly with depth below 300 km (Campbell and Schiffmacher, 1988) that each ring region source current element with less than half-day period (or less than 180° longitude wavelength) can be effectively shielded from some Dst observatories on the Earth's surface.

The ring-current formation model in many researchers' minds is that of Dessler and Parker (1959) who described particle lifetimes from the storm decay phase. Charge exchange, Coulomb collisions and wave-particle interactions were understood to be the dominant causes of the ring-current decay (see reviews by Williams, 1985; Kozyra and Nagy, 1991). Grafe (1988) described the contradictions that arise in the effort to obtain consistent ring-current decay constants from storm data. Roelof's (1989) model of the ring radial and azimuthal currents shows also the generated field-aligned currents. Wrenn (1989) studied the Dst-exponential decays (from 1958 to 1984) and found these to be poor and inconsistent descriptions of the expected processes by which ring-current particles were lost. He said "Dst responds to currents other than RC (ring current); this probably accounts for the many departures from a smooth curve." "...either exponential decay is a poor description of the processes by which particles are lost or there are a number of charge exchange processes with different time constants." The charge-exchange decays in the ring-current region contribute to the conglomerate of fields that are measured by the averaging of data at the Dst observatories. There is some separation of phenomena by the time of occurrence; the compression fields at the initial phase of the classic storm is an example. It may well be that the long tailing-off of the recovery phase after two standard deviations represents a similar time-separation that may eventually be ascribed to the thermospheric, wind-driven dynamo current.

For the ring current associated with a large geomagnetic storm on 6 February 1986, Hamilton *et al.* (1988) computed predicted values of the Dst field during 12 in situ satellite measurements of the ring current. Their table 1 shows that the predicted values of Dst were always less than the observed Dst index and varied from 24% to 84% of the Dst index with an average value of $51.2\% \pm 17.7\%$. These authors suggested possible reasons for the discrepancy, one of which is the presence of other field contributions to the index.

Stormtime, field-aligned currents (Potemera, 1984) connect the disturbed magnetospheric ring currents to the high-latitude ionosphere. The great time variations of the aurora (e.g. periods from 2 s to 200 s) are a visual manifestation of the field-line arrival of the charged particles that contribute to formation of intense auroral electrojet currents. Sun *et al.* (1984) found a considerable field at middle latitudes from the auroral-region field-aligned currents. These authors made their computation of field effects for Dst observatory locations at Honolulu and San Juan, as well as at the Tucson observatory (which is located at a lower Gustaffsson model geomagnetic latitude than the Dst index observatory at Hermanus, South Africa). They determined (see Abstract) that "in agreement with earlier studies, the field-aligned current segments have, in general, the largest contribution to both the *H* and *D* components in middle latitudes." Thus, in the present method that is used to represent the storm field and Dst by *H* components, the field-aligned currents may be the largest contributors.

Storm-field changes are enhanced at the narrow regions of the equatorial electrojet in daytime. Rastogi and Patil (1986) illustrated this fact with a comparison of the field sizes at Trivandrum and Alibag Indian observatories. Such an enhancement is one of the reasons for the equatorial exclusion of Dst observatory locations for Dst. The enhancement is due to an E-region ionospheric conductivity amplification over the dip equator. The currents arrive there only through the mid-latitude ionosphere and must originate from the auroral electrojet currents prevailing at storm times. Dst stations at mid-and low-latitude locations, therefore, must be sensitive to such overhead ionospheric currents.

The expected quiet-day ionospheric dynamo current field, Sq, is subtracted from the station observations in the daily Dst index preparation. Values for this subtraction are obtained from the five most undisturbed-day records in the same month. The dynamo current depends upon the E- and lower F-region ionospheric conductivity, as well as the transport of ionization by tidal and thermospheric wind forces. During a geomagnetic storm, both the ionosphere (Davies, 1989) and the thermospheric wind system (Blanc and Richmond, 1980) are severely disturbed. The actual dynamo current system during a storm, as seen in the *H*-component of field, is greatly different from the quiet-day levels that are subtracted in the index formation. As a result, the Dst contains significant field values that are the difference between the five-quiet-day-level and the storm-time Sq.

All these ionospheric and magnetospheric currents at storm time (field-aligned, ionospheric, ring, tail, boundary, etc.) are adding to the mid-and low-latitude observed fields at the Earth's surface. The relative contributions must vary greatly with station location and storm time. An average of these *H*-component fields at selected observatories becomes the Dst index. Nevertheless, the myth that the negative storm-time Dst field values represent a ring-current growth and decay has continued as a simple, but questionable, explanation of the geomagnetic storm main and recovery phase shape.

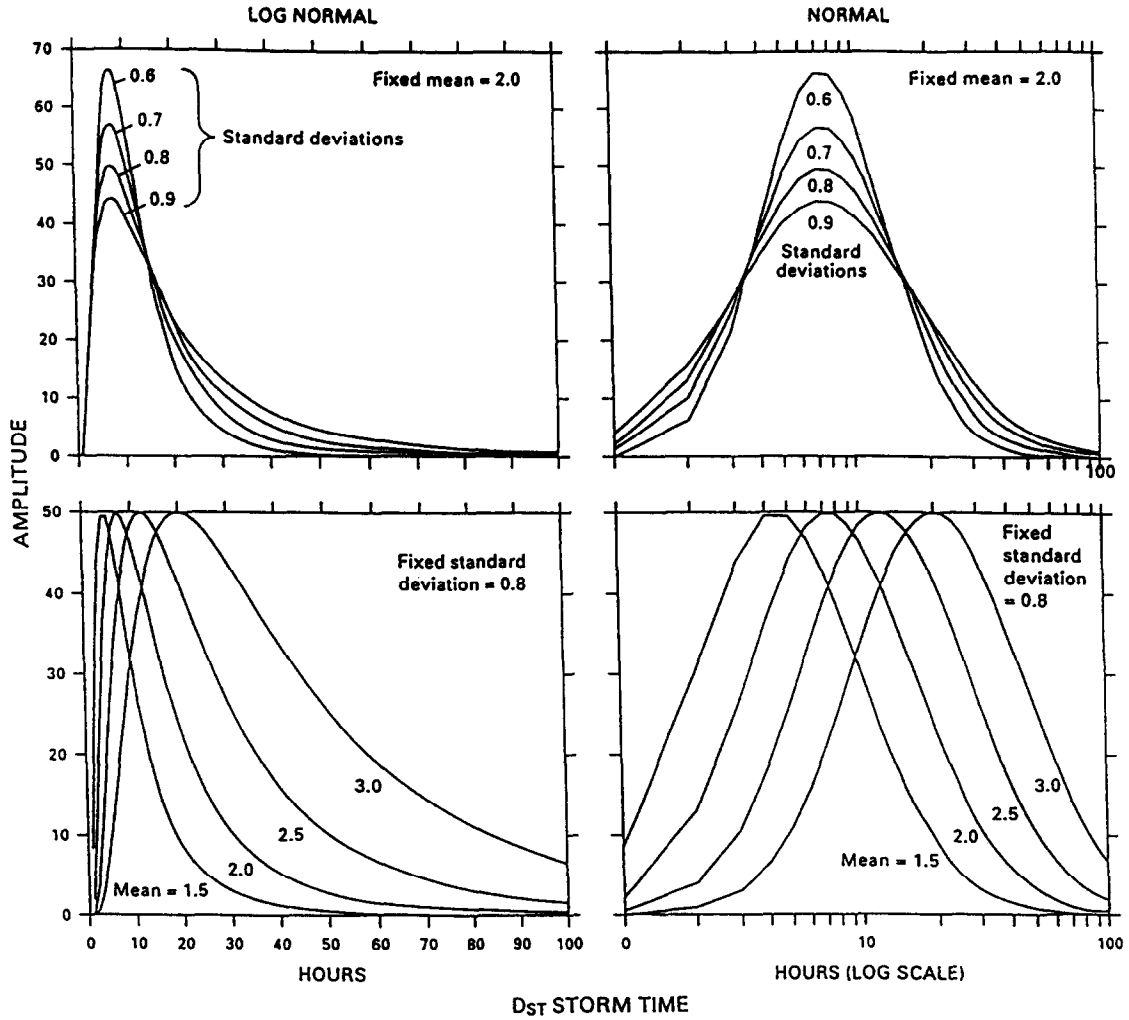

Fig. 3. Lognormal distribution functions for fixed mean (top) and fixed standard deviation (bottom) using typical geomagnetic storm values. Note the log-time scale for the X-axis of the two figures at the right.

3. LOGNORMAL DISTRIBUTION CHARACTERISTICS

If a normal distribution results from the plotting of the logarithm of the independent variable measured for a statistical feature, the probability distribution is said to be lognormal. Aitchison and Brown (1957) produced the most detailed review of this subject. The material in this section was gleaned primarily from their textbook, referred to hereafter as 'A and B'. Following A and B, the lognormal distribution of the variable x will be designated as $A(x|\mu, \sigma^2)$ or, more simply, $A(x)$, where μ is the mean of the logarithms of x, and σ^2 is the variance ($\sigma = \sqrt{\sigma^2}$ is the corresponding standard deviation). Figure 3 shows two families of lognormal probability distributions, for fixed μ and for fixed σ, where the ranges of μ and σ were selected to match the ranges of such values in the storms to be presented in the following section. Here, x is the duration of time in hours. Note, in particular, how the positive skewness of the distribution increases to the right, rapidly, with increasing μ.

The lognormal distribution is a common feature in nature. The formula for this distribution (with $x > 0$) is:

$$A(x) = \frac{1}{\sigma\sqrt{2\pi}} \exp\left[-\frac{1}{2}\left(\frac{\ln(x)-\mu}{\sigma}\right)^2\right],$$

where $A(x)$ is the distribution size of the variate. Note that $\lim_{x\to 0+} [A(x)] = 0$. The lognormal form arises primarily from two situations: (1) when the distribution size of the variate can "be regarded as the

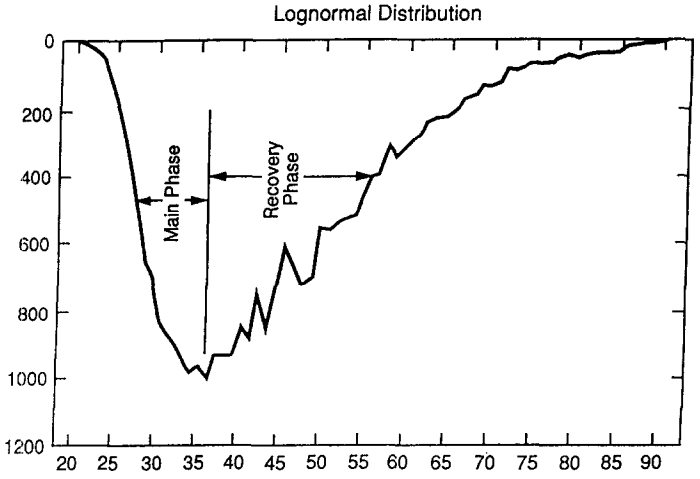

Fig. 4. Ages of AGU membership, redrawn from the AGU Membership Directory, p. 3, 1991; this is a typical lognormal distribution. The figure is plotted with the X-axis as age and the Y-axis as number of members; the number increases downward to show similarity to the form of a geomagnetic storm that would be labeled 'main phase' and 'recovery phase'.

joint effect of a large number of mutually independent causes, acting in ordered sequence during the time of growth"; or (2) there are multiple causes, not necessarily in order of sequence, e.g. when "we may suppose that at any point of time the existing distribution of the variate arises from a large number of causes which operate simultaneously" (A and B). Examples of lognormal distributions are (Koch and Link, 1980): gold assays, magnitudes of earthquakes, heights of floods in a river and heights of buildings in New York City. Other examples are (A and B): annual income size distribution in a population, levels of organism tolerance to drugs, prices paid per unit of a commodity by individual families, body weights of human beings, final size of biological organisms, distribution of households by numbers of resident persons, effective life of an industrial material, distribution of stars, ages of men and women at their first marriage, and frequencies with which authors use nouns. Figure 4 shows a lognormal distribution of the ages of the members in the American Geophysical Union. The Y-axis has been inverted to illustrate the similarity to a typical Dst storm.

Three items of importance discussed by A and B concerning the variate X are zero values, displacement and truncation. For the lognormal distribution, X can only assume values greater than 0 if we wish to form the equivalent normal distribution display. That is not a problem for the variate representing time from the beginning of an analyzed statistical event. If the exact start (threshold or lower bound) at $x = b$ can be estimated on a priori grounds, a new variate is formed $x' = x - b$ (as a simple scale translation) in place of X; the new variate, x', has all the properties of the usual lognormal distribution. If the measurements have an ending (truncation or upper bound) at $x = e$, which also can be determined a priori, then A and B suggest using a new variate $x' = (x-b)/(e-x)$ for $x > e$. Another method for treating the wings of the distribution might be to ignore values outside several standard deviations of the mean.

The statistical behavior of Dst (as a number of hourly values of negative Dst in 2-gamma bins) has been published for samples of quiet (1965) and active (1958) years by Campbell (1979). These distributions show the typical lognormal statistical form. Such a form is expected because of the many contributions to the Dst measurement and the connected series of statistical processes that give rise to the low-latitude fields.

4. GEOMAGNETIC STORMS AS LOGNORMAL DISTRIBUTIONS

It was recently noticed (Campbell, 1993) that the typical storm-time Dst index also follows a lognormal profile in the time-series domain (usual amplitude plot). Each ionospheric and magnetospheric process contribution to Dst has its own characteristic time-series distribution; when added to form Dst, a lognormal time-series distribution results. The lognormal form can be simply verified by a transformation to the log-time domain and computation of the usual normal-form data fitting tests. The symmetry of the

Table 1.

Storm no.	Date	Maximum (γ)	Total* (γ)	μ mean	σ std. dev.	% Fit variation†
1	16 Feb 1967	130	3125	1.999	0.893	12.3
2	10 Mar 1979	140	2741	2.188	0.805	13.6
3	13 Jan 1967	160	3724	2.355	0.756	7.9
4	18 Apr 1965	162	2114	1.804	0.836	24.0
5	19 Dec 1980	240	4387	2.048	0.742	7.8
6	5 Sep 1982	289	8354	2.588	0.868	9.3
7	9 May 1992	297	7255	2.981	0.617	18.3
8	8 Nov 1991	354	8318	2.586	0.792	14.7
9	11 Feb 1958	426	7220	2.163	0.718	12.9
10	13 Sep 1957	427	6866	2.200	0.773	22.8
						av. 14.3 ± 5.7

*Within mean ± two standard deviations.
†Start to 3 × peak hour.

bell-shaped (normal) curve about the mean, maximum amplitude, position tells us that the fall of the curve from its maximum can be predicted from its initial rise to maximum. Transforming this prediction back to the linear-time domain means that observations made during the first few hours of storm Dst rise-to-maximum allow us to predict field levels for the many hours of the storm Dst recovery period.

Table 1 lists 10 geomagnetic storms that were analyzed for lognormal characteristics. These storms were selected from the readily available literature, requiring only that there be a distribution of sizes at the maximum excursion of the main phase. Field values for the storms were obtained from the World Data Center A listing of Dst hourly indices. Paired storms 3 and 4, as well as 9 and 10 were chosen to see if storms of similar peak value yielded similar lognormal characteristics. They did not. In many cases, the storm onset (hour 1) was taken to be the first small negative field value of Dst (storms 1, 3, 4, 9, 10). This start time was difficult to determine when the storm occurred in the midst of generally disturbed conditions. For such cases (storms 2 and 6), I selected the start as the smallest numerical value of negative Dst just before the obvious major excursion of the main phase. For two storms (5 and 8), to see the impact of the beginning hour selection, I assumed the start to be at the hour just before the start of the major negative excursion, and I assigned the start an amplitude of 0.01 gamma (1 gamma = 1 nano Tesla). As noted in the preceding section, translation of the time axis would not affect the basic lognormal characteristics. The sometimes-present initial phase of positive Dst certainly interferes with accurate selection of the hour for main-phase beginning. The end-time of the storm was arbitrarily taken to be 50 hours after the start, except for storm 5 which entered a second disturbed period after 38 hours. The truncation formulation of the variate (time) suggested by A and B was not attempted for this test of the storm lognormal distribution.

The left columns in Fig. 5 and Fig. 6 show the 10 storms arranged (top to bottom rows) in order of increasing storm peak amplitude. The negative Dst values are plotted positively in hours from the start time in this real-time domain. Note the changing amplitude scales to the right. The center columns in these figures show the 10 storms plotted as the natural logarithm of duration time versus Dst amplitude in the log-time domain.

Using evenly spaced values from the extrapolated amplitudes in the log-time domain, the best fitting normal distribution was determined, having a characteristic mean, μ, and standard deviation, σ (listed in Table 1). The dashed curves in the center columns of Fig. 5 and Fig. 6 represent the resulting normal distribution curves. Note how well the storm values follow the normal shape in the log-time domain. Next, these normal curves are transformed back to the natural-time domain and plotted as dashed lines with the left column representations of the Dst storms. The percent absolute difference between the lognormal curve and the storm values was computed. Then, these percentages for hourly measurements from the storm start to three times the peak hour were averaged and shown in the last column of Table 1 as a measure of the lognormal fitting. For the 10 storms, the average fit to lognormal was 14.3 ± 5.7%. A third characteristic of storm lognormal distributions is the area under the curve. To represent this, I sum the hourly gamma field values that occur within ± two standard deviations of the mean (Table 1).

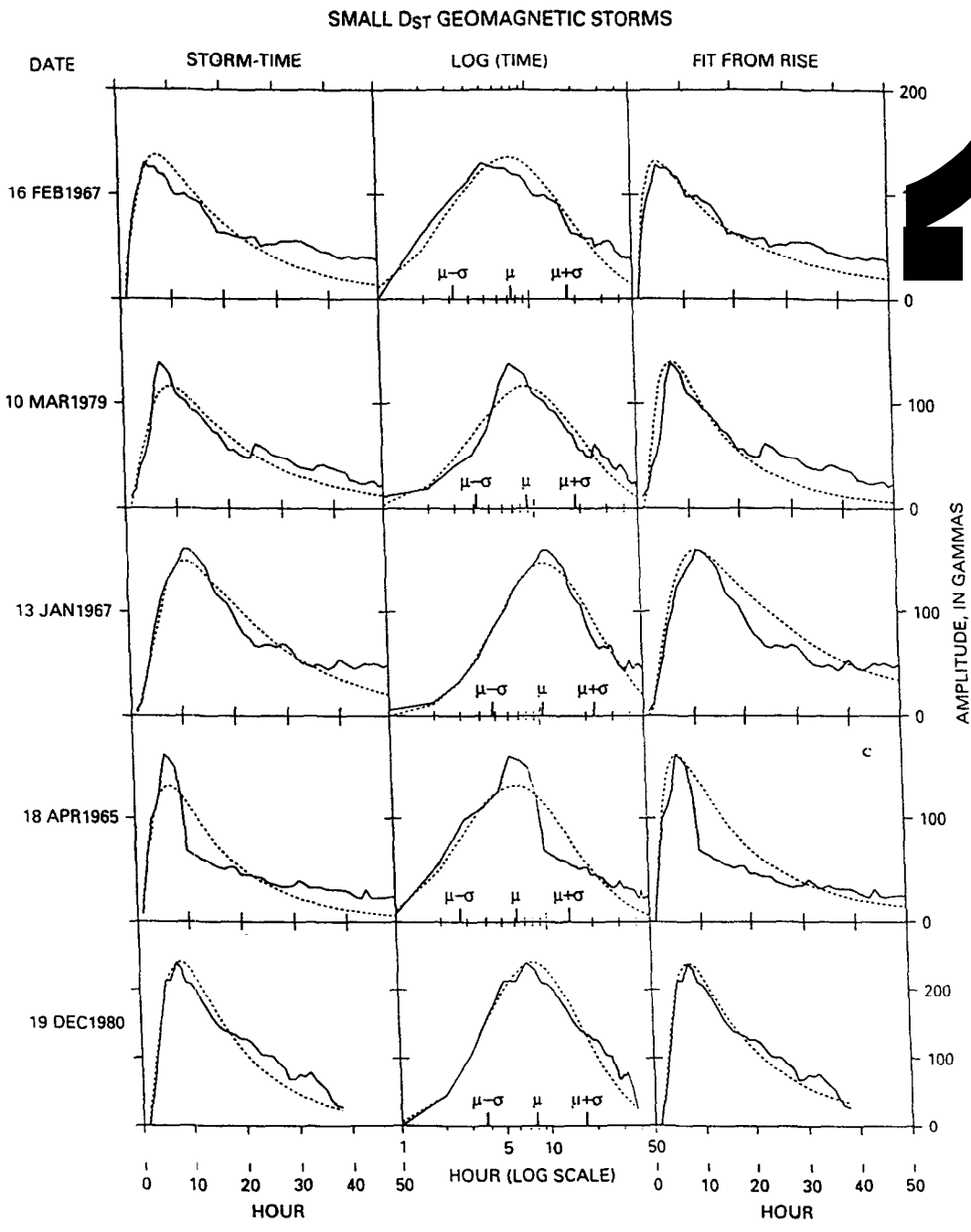

Fig. 5. Small Dst geomagnetic storms, under 250 gamma in maximum values. The indices were obtained from World Data Center A, Boulder, Colorado, U.S.A. Storm dates are identified to the left. In the left column, the solid line is the absolute value (Y-axis) of the Dst for the main and recovery phases in storm time (X-axis); the dashed line is the best-fitting lognormal distribution for each storm. In the center column, the Dst values are replotted (solid line) on a log-time (X-axis) scale; the dashed lines show the best fitting normal distribution curve; the mean, μ, and standard deviation locations, $\mu \pm \sigma$, are indicated. In the right column, the solid line is a repetition of the storm representation of the left column, whereas the dashed line is the lognormal storm fit value obtained from a recovery-phase prediction program using only the storm values of the main phase plus one point past the storm peak.

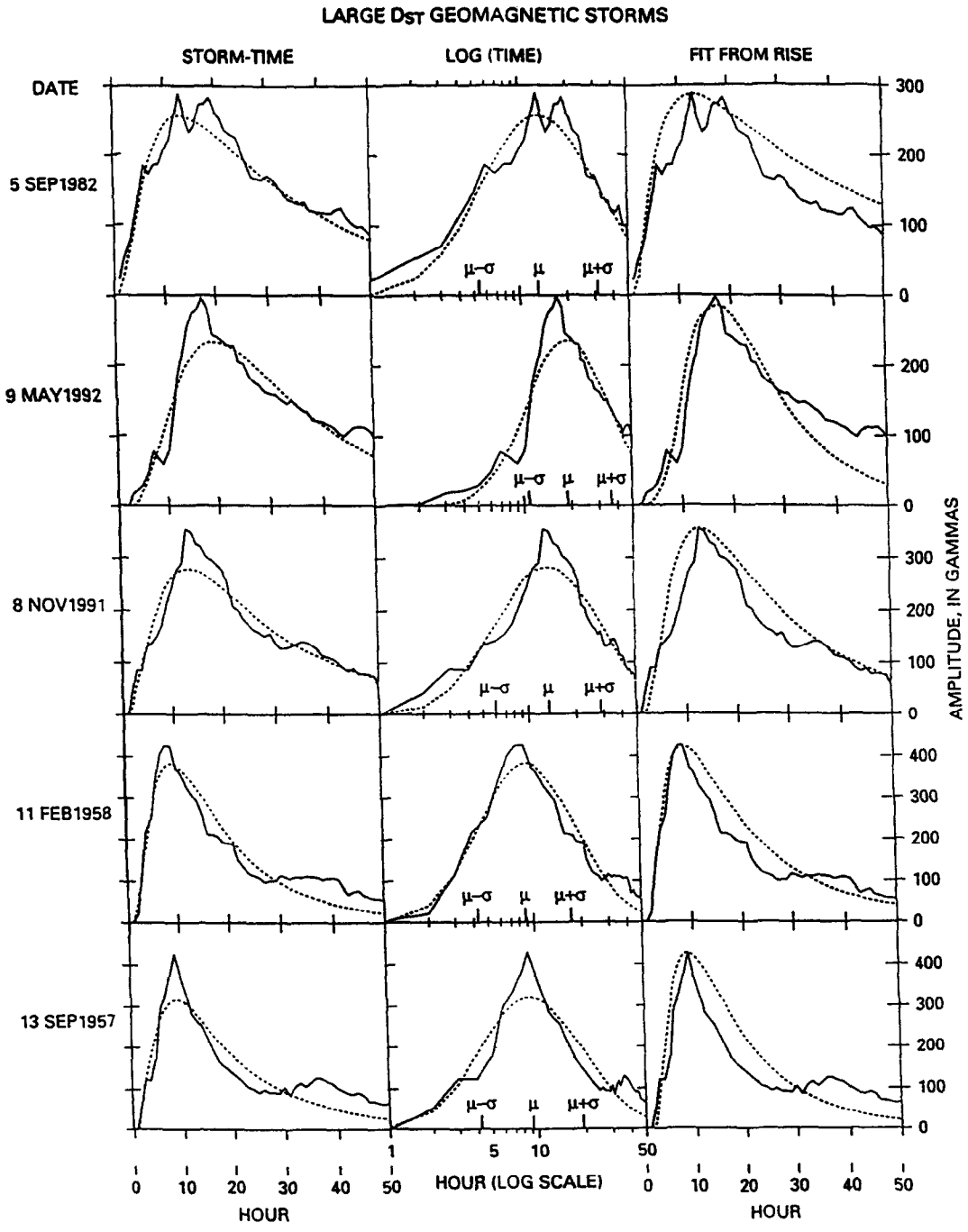

Fig. 6. Same as Fig. 5, only for large Dst geomagnetic storms reaching above 250 gamma in size.

Only four observatories presently contribute to the Dst values used in the above studies. With more observatories, the Dst forms become considerably smoother, and I believe that they would become even closer to the lognormal form. The lognormal representation also might be improved by adjustment

for magnetospheric compression (+Dst of the initial phase) and for truncation (A and B) of the storm sample. The storm characteristic means and standard deviations are not functions of the peak amplitudes. If the 10 storms had been grouped by size and then averaged as in the early Sugiura and Chapman (1960) analysis, the characteristic μ and σ storm values would have been destroyed.

5. NEW VIEWPOINT FOR STORMS

The lognormal distribution seen in the quantity of papers produced by scientists has been ascribed to the dependence on the numerous factors leading to final publication (West and Shlesinger, 1990). In keeping with that finding, I propose an analogy to help visualize the storm distribution function. Consider an international meeting of various geophysical disciplines (e.g. IUGG). At the end of this meeting, the participants are asked to make a very special effort to see that their oral and poster presentations are subsequently published in a scientific journal of their own selection. Time delays occur because there is a sequence of processes involved—a statistical distribution of those who wish to start the writing, a distribution of time at the writer's organization in getting the manuscript physically ready, a distribution of time due to the review process, a distribution due to the particular journal's processing procedures, etc. Renowned scientists, selected as observers to represent each of the major geographical areas, are asked to follow and record the average number of articles published (by the meeting attendees) at each date, counting from the meeting end. The observers do not have a list of meeting attendees, so each depends on various local sources of information. The counts of number of publications versus time from the meeting are biased by the speciality of each observer and by his (or her) geographic location. The counts of some publications are duplicated by the different observers. After two years (730 days), the data gathered by the observers are averaged by day of publication from the meeting end. The distribution of counts, $A(t)$, versus time, t, is lognormal. We then plot the number $A(t)$ versus $\ln(t)$ and obtain the characteristic mean, standard deviation and hours of two standard deviations from the mean. Using the same observers for other meetings, the characteristic values of importance are the normal curve mean and standard deviation, as well as the apparent total number of publications between the two standard deviation limits.

With this analogy, we can think of the storm-time negative Dst values as proportional to the count of field contributions at each hour into the storm. The count is an average from observations at four locations distributed at middle and low latitudes about the Earth. One observatory's storm-time measurements are a representation of the ensemble of individual field contributions from a limited number of substorm sources (e.g. field-aligned currents, ring currents, tail currents and ionospheric currents). The characteristic variation periods of each contributing source field are short with respect to the duration of the storm Dst. At each time sector of the Earth, the proportional contribution of each source can change. Any one of these substorm sources is caused by the joint effect of a large number of physical processes acting in ordered sequence (e.g. solar wind, to southward turning field, to field line merging, to tail energization, to...etc.).

The question that immediately arises is "Why hasn't the lognormal fitting of Dst come to light before now?" It has been 85 years since the Moos (op cit.) publication. I can think of a few possible explanations that may range from incidental to quite apparent. (1) The first detailed textbook (A and B) on lognormal distributions did not arrive on the scientific scene until 1957, in a period that was dominated by the start of the International Geophysical Year, the initiation of satellite research, and the discovery of radiation belts encircling the Earth. Geophysical scientists of the time, who may have envied the beauty of Saturn's rings, hoping to find a similar Earth-bound feature, encouraged the Dst ring-current explanation of storm fields. (2) Sydney Chapman, who dominated the thinking on geomagnetism from early this century until his death in 1970, seemed to be unhappy with Birkeland's field-aligned currents (cf. Dessler, 1984) and favored averaging large data sets to establish quasi steady-state equivalent currents as opposed to treating of each event separately (Stern, 1991). Chapman, as the student Sugiura's Ph.D. advisor, was instrumental in the identification of Dst as a ring-current index. (3) Positive and negative charge and field definitions are arbitrary. For example, the Chinese selected southward as the definitive direction for the first compass. If our storm fields were plotted in the positive direction, the lognormal feature would have been more obvious.

6. DST RECOVERY—PHASE PREDICTION

There is some utility in the fact that Dst storm representations from the ensemble of middle- and low-latitude stations follow a lognormal shape. In the log-time domain, we have seen that these storms have a

normal distribution shape. For the bell-shaped (normal) profile, field values from the onset and rise to the mean (at storm maximum) positions are mirrored by the fall to the distribution end. In other words, within determined error limits, information on the shape following the peak is contained in the rise to peak value. This behavior, translated to the realtime domain of the storm Dst, signifies that a knowledge of the storm recovery phase can be obtained from the growth phase, within definable error limits.

To illustrate this predictability, I used the Dst values for the 10 storms of Table 1. I selected absolute values of the hourly Dst indices starting from the negative Dst onset until the peak was passed at one hour following the end of the growth phase. The average value of the peak and the first value following the peak was taken to be the size of the maximum. I then performed a regression fit to this storm main-phase data using a nine-term polynomial function. With this polynomial, I determined evenly spaced field values in the log-time domain. Assuming the maximum to be located at the mean, I then folded the values to obtain the full expected distribution, and I determined a standard deviation of the assumed normal curve. The equivalent real-time, full-storm (lognormal) distribution was then found from these characteristic constants and plotted as a dashed curve in the right columns of Figs 5 and 6. The solid curve shows the actual Dst values. As a goodness-of-fit measure, I computed the percent differences [100 (observed − predicted)/observed] for hourly values from the peak time to three times the peak time. The averages of these percentages for the storms showed that I was able to predict the storm recovery phase values to 25.7%. This prediction procedure could be refined, for example by making allowance for initial phase compression and for truncation. With periodic prediction readjustments during the storm progress, the limiting fit would reach the lognormal representation shown in the left columns of Figs 5 and 6.

7. CONCLUDING REMARKS

The recognition of a typical form for the averaged low- and middle-latitude geomagnetic disturbance events has had a long history of development from the first discovery by Moos in Bombay at the beginning of this century. At the onset of space research, Chapman's attractive representation of the storm field as a ring of current encircling the Earth grew in favor, supported by the statistical satellite evidence of a special storm-time distribution of charged particles in the region of about 3–9 *Re* (Earth radii). Chapman's propensity for always representing averaged fields as distant current systems was unquestioned. A special activity index Dst, which was standardized in this period and designated as the 'Ring-Current Index,' has continued to be produced and similarly identified even now. For a great many years, the ring model simplicity has encouraged use of this index (and use of observatory records organized in similar fashion) to be applied to a variety of research endeavors. Among these are: (a) corrections to main field (global mapping) data for magnetospheric disturbance interference; (b) adjustments of the size determinations for the equatorial ionospheric electrojet current; and (c) use of the derived ring-current source for probing Earth-mantle electrical conductivity. The identification of the storm with the simple magnetospheric ring current is so universally useful that questions regarding its validity have been almost completely ignored.

By the mid 1900s, when the 'geomagnetic storm' was equated to the Dst index representation, early indications of some problems with that assumption were avoided as the research focus shifted to substorms—a collection of solar–terrestrial disturbance processes that culminate in the appearance of auroras (cf. review by McPherron and Baker, 1993). Satellite observations allowed substorm processes to be tracked from their initiation at the southward turning of the interplanetary magnetic field (as the solar wind encountered the Earth's main field) to the final high-latitude surface manifestation when field-aligned energetic particles precipitated into the upper atmosphere. Recent process reconstruction studies showed that fields from the various substorm related mechanisms should be of significant size at low latitudes on the Earth. Ring-current region observations indicate that short-duration, substorm-like, partial-ring processes prevailed during the disturbed period; there was insufficient current in the ring region to cause all the Dst fields; there was no decay corresponding to the surface fields. The picture of a main-phase rise to maximum and recovery phase decay of ring particles paralleling the Dst changes is a myth.

It has been reported here that the Dst index representation had a lognormal form. Such profiles transform to simple normal distributions. The three characteristics of a bell-shaped normal distribution are its mean, standard deviation and the area under the curve. Thus, two parameters for describing Dst-storm shape properties are the mean and standard deviation of the storm plotted in the lognormal domain. The third parameter, the size property, can be identified with the sum of the measured field values within the time between two standard deviation limits

(cf. Table 1). Such a storm size representation has a general correspondence to the classical division into small and large storms listed by the maximum attained field amplitude at the end of the main phase (the 1–10 original ordering of the events). Note, however, that, with the area ordering, the largest two storms are numbers 6 and 8, and the smallest are numbers 2 and 4. In the lognormal representation, similar storms must have similar total size, μ and σ. With such an interpretation, storms 6 and 8 are similar. Traditionally, storms have also been classified into 'recurrent' and 'non-recurrent' types, as well as 'directly driven' and 'loading/unloading' types. If there is a reflection of this difference in lognormal storm characteristics, it might possibly be seen in μ and σ.

Our knowledge that the expected form of the storm Dst has a normal distribution shape in the log-time domain allows a forecast of the storm recovery phase amplitudes to be made from the measurements during the storm main phase. Preliminary tests of the predictability produce the good results indicated in the right column of Figs 5 and 6. The results are better than those found in the recent attempts to correlate the storms with ring currents. A copy of the prediction program for desk-top PCs is available from the author upon request.

Figure 7 describes lognormal distribution formations. The upper left column illustrates how marbles dropped through a funnel to a regular distribution of pins can be collected in bins. The count of marbles at each bin position describes a normal (bell shaped, Gaussian) distribution. The funnel central position and pin arrangement fix the distribution mean and standard deviation; we can call these two the 'source distribution mechanism'. For sequential sources (top central column) in which a first source distribution mechanism occurs, and then the results undergo a second distribution mechanism, and then these results follow a third mechanism, etc., the final counts, Y, found at the X-bin positions produce a lognormal shape. Similarly, simultaneous source distributions (top right column of the figure) will also produce Y numbers at the X positions that follow a lognormal shape. Lognormality is verified by a plot of $\ln(X)$ versus Y (lower right in the figure) showing a bell-shaped distribution. The lognormal distributions vary as in the lower left corner of the figure. For low-latitude geomagnetic disturbances consider that the collection bins are arranged in positions at hourly intervals from the storm onset to its demise. In each hour-bin we add the fields from different observatories and different source distribution mechanisms (whether operating sequentially or simultaneously) that rise to a maximum and dissipate individually during the storm lifetime. The collection bins cannot know that the classical statistical is replaced by a time series. Fields are added at the time-bins in a fashion paralleling the marble collection at position-bins.

I believe that the Dst time series is lognormal in form because each of the various time series that compose it has its own characteristic amplitude-time distribution form; the summation of such distributions is, by A and B standards, lognormal in form. Whatever the cause, it is striking that a form, closely adhering to a lognormal shape, occurs for the storm Dst. This form and the Dst magnitudes cannot be explained by fields in the ring-current region of the magnetosphere. Application of the lognormal shape allows reasonable prediction of the storm recovery phase from the observation of only the storm growth phase. Presently, it seems very likely that an explanation of the storm Dst shape lies in the statistical features of the index.

One might question why other indices such as Kp (or its linear form Ap) and AE do not have the lognormal shape in the time domain. AE is dominated by just one process, the auroral region field-aligned currents and their closing current system in the auroral ionosphere. Ap (and Kp) indices are similarly dominated; the linear correlation coefficient between AE and Ap is 0.89 (Campbell, 1979) because of the high-latitude locations of the contributing stations. What makes Dst a useful disturbance index is the diversity of the many current processes that fashion the measurements. I believe that it is also this diversity that is responsible for the lognormal shape in the time domain.

The new interpretation of the cause of the Dst geomagnetic storm 'main phase' and 'recovery phase' will probably find support from substorm researchers. The interpretation of external and internal fields, separated from Dst-type measurements in a spherical harmonic analysis, will need re-examination because the source is not a simple ring current. The significance of the simple asymmetric (partial) ring-current representation of the surface storm fields should also be reconsidered. Main field modelers with satellite-derived data may question the application of Dst corrections to their observations. Storm-related phenomena may need reinterpretation. Although I believe that the International Association of Geomagnetism and Aeronomy Working Group on Indices should officially announce an end to the mythical identification of Dst as the 'Ring-Current Index', the established use of Dst as a world-wide indicator for geomagnetic disturbances is too valuable to bury by this new 'lognormal' understanding.

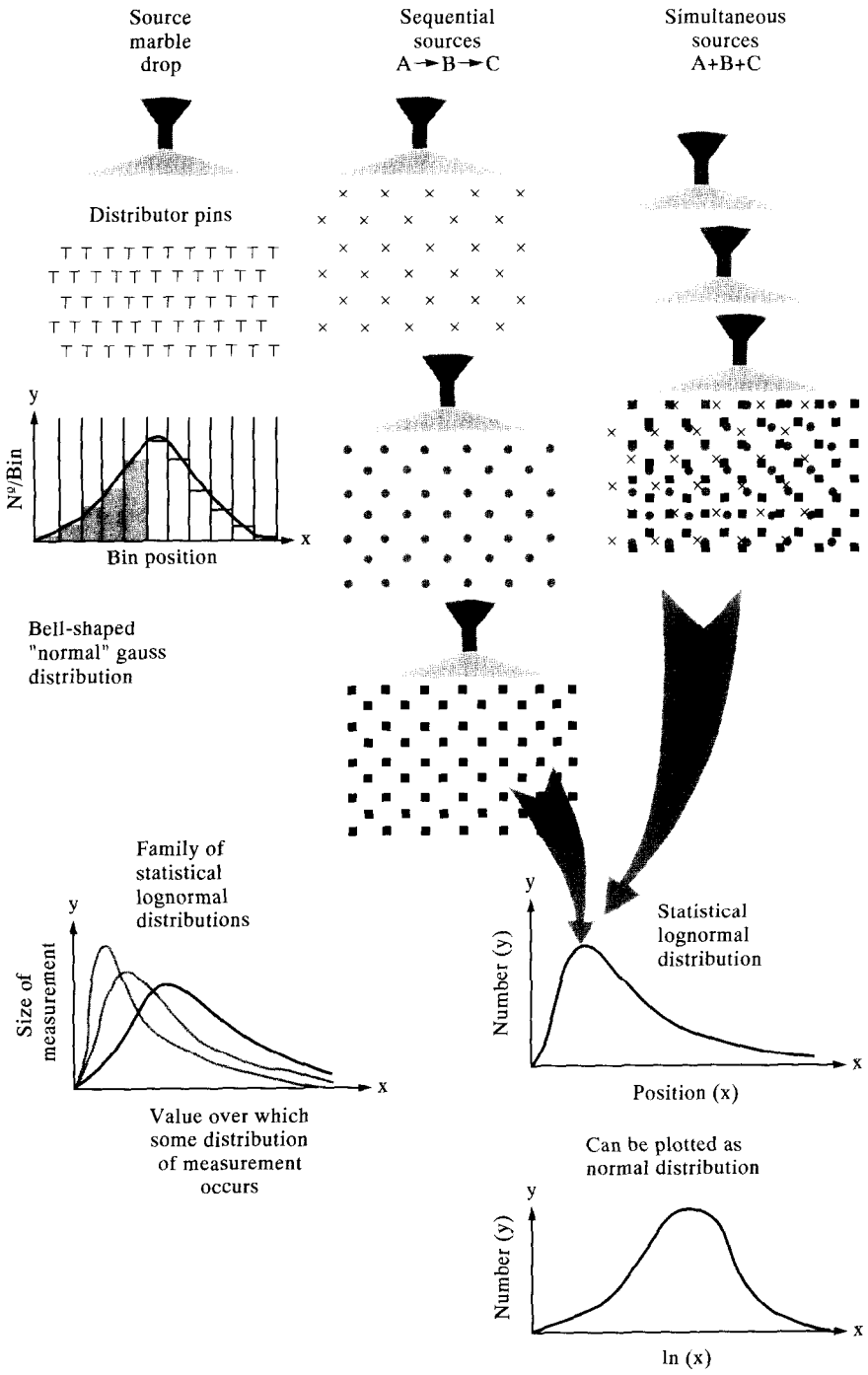

Fig. 7. A diagram describing the formation of lognormal distributions (see text).

Acknowledgement—This paper is an elaboration of an oral presentation originally given at the NOAA Laboratory in Boulder, Colorado, on 9 October 1992. The work was supported, in part, by the U.S. Naval Oceanographic Office. The World Data Center A provided the storm-time indices and encouraged the investigation. Figure 7 was prepared for me by the Australian Geological Survey Organisation. I thank the numerous colleagues who, upon receiving the original manuscript, offered many constructive suggestions.

REFERENCES

Aitchison J. and Brown J. A. C. 1957 *The Lognormal Distribution with Special Reference to its Use in Economics*, Cambridge University Press, 176 pp.

Akasofu S. I., Cain J. C. and Chapman S. 1961 The magnetic field of a model radiation belt, numerically computed. *J. geophys. Res.* **66,** 4013–4026.

Akasofu S. I. and Chapman S. 1961 The ring current, geomagnetic disturbance and the Van Allen radiation belts. *J. geophys. Res.* **66,** 1321–1350.

Akasofu S. I. and Chapman S. 1964 On the asymmetric development of magnetic storm fields in low and middle latitudes. *Planet. Space Sci.* **12,** 607–636.

Akasofu S. I. and Chapman S. 1972 *Solar–Terrestrial Physics*, Oxford University Press, London, 901 pp.

Akasofu S. I., Chapman S. and Venkatesan D. 1963 The main phase of great magnetic storms. *J. geophys. Res.* **68,** 3345–3350.

Allen J., Frank L., Sauer H. and Reiff P. 1989 Effects of the March 1989 solar activity. *EOS, Trans. Amer. Geophys. Un.* **70,** 1479–1488.

Blanc M. and Richmond A. 1980 Ionospheric disturbance dynamo. *J. geophys. Res.* **85,** 1669–1686.

Campbell W. H. 1973 Field levels near midnight at low and equatorial geomagnetic stations. *J. atmos. terr. Phys.* **35,** 1127–1146.

Campbell W. H. 1979 Occurrence of AE and Dst geomagnetic index levels and the selection of the quietest days in a year. *J. geophys. Res.* **84,** 875–881.

Campbell W. H. 1984 An external current representation of the quiet nightside geomagnetic field level changes, *J. Geomag. Geoelectr.* **36,** 257–265.

Campbell W. H. 1993 Storms, log-normal distributions, and Dst ring current, Paper 3 presented at Session 3.15 of 7th Scientific Assembly of IAGA, Buenos Aires, 10 August.

Campbell W. H. and Schiffmacher E. R. 1988 Upper mantle electrical conductivity for seven subcontinental regions of the Earth. *J. Geomag. Geoelectr.* **40,** 1387–1406.

Celsius A. 1749 Anmerkungen über die stündlichen Veränderungen der Magnetnadel. *Svensk Vet. Acad. Handl.* Hamburg **2,** 45–48.

Chapman S. 1919 An outline of a theory of magnetic storms. *Proc. Roy. Soc. London* **A-95,** 61–83.

Chapman S. 1927 On certain average characteristics of worldwide magnetic disturbances. *Proc. Roy. Soc. London* **A-115,** 242–267.

Chapman S. 1935 Electric current systems of magnetic storms. *Terr. Mag. and Atmos. Electr.* **40,** 349–370.

Chapman S. 1951 *The Earth's Magnetism*, John Wiley, New York, 127 pp.

Chapman S. and Ferraro V. C. A. 1932 A new theory of magnetic storms, Part I. The initial phase. *Terr. Mag. and Atmos. Electr.* **36,** 77–97 and 171–186, 1931, and **37,** 147–156 and 421–429.

Cummings W. D. 1966 Asymmetric ring currents and the low-latitude disturbance daily variation. *J. geophys. Res.* **71,** 4495–4503.

Davies K. 1989 *Ionospheric Radio*, Peter Peregrinus, London, 580 pp.

Dessler A. J. 1984 The evolution of arguments regarding the existence of field-aligned currents, in *Magnetospheric Currents* (Edited by Potemera T.A.), Geophys. Monogr. Vol. 28, pp. 22–28. Amer. Geophys. Un., Washington, D.C.

Dessler A. J. and Parker E. N. 1959 Hydromagnetic theory of geomagnetic storms. *J. geophys. Res.* **64,** 2239–2252.

Forbush S. E. and Casaverde M. 1961 The equatorial electrojet in Peru, Carnegie Inst., Washington, D.C., Pub. 620.

Frank L. A. 1967 On the extraterrestrial ring current during geomagnetic storms. *J. geophys. Res.* **72,** 3753–3767.

Fukushima N. and Kamide Y. 1973 Partial ring current models for worldwide geomagnetic disturbances. *Rev. Geophys. Space Phys.* **11,** 795–853.

Grafe A. 1988 The influence of the recovery phase injection on the decay of the ring current. *Planet. Space Sci.* **36,** 769–773.

Graham G. 1724 An account of observations made of the variation of the horizontal needle at London, in the latter part of the year 1722, and beginning of 1723. *Phil. Trans. Roy. Soc. London* **A-32,** 99–107.

Hamilton D. C., Glockler G., Ipavich F. M., Studemann W., Wilken B. and Kremser G. 1988 Ring current development during the great geomagnetic storm of February 1986. *J. geophys. Res.* **93,** 14343–14355.

Hoffman R. A. and Bracken P. A. 1967 Higher order ring currents and particle energy storage in the magnetosphere. *J. geophys. Res.* **72,** 6039–6049.

Kamide Y. 1979 Relationship between substorms and storms, in *Dynamics of the Magnetosphere* (Edited by Akasofu S.I.), pp. 245–443. D. Reidel, London.

Kertz W. 1964 Ring current variation during the IGY, in *Ann. Int. Geophys. Year*, Vol. 35, p. 49. Pergamon Press, Oxford.

Koch Jr, G. S. and Link R. F. 1980 *Statistical Analysis of Geological Data*, Vol. 1, 375 pp. Dover, New York.

Kozyra J. U. and Nagy A. F. 1991 Ring current decay-coupling of ring current energy into the thermosphere/ionosphere system. *J. Geomag. Geoelectr.* **43,** Suppl., 285–297.

Lui A. T. Y., McEntire R. W. and Krimigis S. M. 1987 Evolution of the ring current during two geomagnetic storms. *J. geophys. Res.* **92,** 7459–7470.

McPherron R. L. and Baker D. N. 1993 Factors influencing the intensity of magnetic substorms. *J. atmos. terr. Phys.* **55,** 1091–1122.

Matsushita S., Tarpley J. D. and Campbell W. H. 1973 IMF sector structure effects upon the quiet geomagnetic field. *Radio Sci.* **8,** 963–972.

Mayaud P. N. 1980 Derivation, meaning, and use of geomagnetic indices. *Geophys. Monogr.* **22,** Amer. Geophys. Un., Washington, D.C., 154 pp.

Moos N. A. F. 1910 Magnetic observation made at the government observatory for the period 1846–1905, Part II, Ch. X (see Chapman, 1919).

Potemera T. A. 1984 Magnetospheric currents. *Geophys. Monogr.* **28,** Amer. Geophys. Un., Washington, D.C., 357 pp.

Rastogi R. G. and Patil A. R. 1986 Complex structure of equatorial electrojet current. *Curr. Sci.* **55,** 433–436.

Roelof E. C. 1989 Remote sensing of the ring current using energetic neutral atoms. *Adv. Space Res.* **9,** 195–203.

Rostoker G. 1993 Magnetospheric substorms—their phenomenology and predictability, Solar Terrestrial Predictions—IV, Proceedings of Workshop at Ottawa, Canada, May 1992, NOAA U.S. Dept. of Commerce Pub., Vol. 3, pp. 21–35.

Schmidt A. 1917 Erdmagnetismus, Enzyklopaedie der Mathematischen Wissenschaften, Band VI, Leipzig (see Akasofu and Chapman, 1961).

Singer S. F. 1957 A new model of magnetic storms and aurorae. *EOS, Trans. Amer. Geophys. Un.* **38,** 175–190.

Stening R. J. 1990 A lunar tide in the Dst index. *J. Geomag. Geoelectr.* **42,** 11–17.

Stern D. P. 1991 The beginning of substorm research, magnetospheric substorms. *Geophys. Monogr.* (Edited by Kan J. R., Potemra T. A., Kokubun S. and Iijima T.), Vol. 64, pp. 11–14. Amer. Geophys. Un.

Sugiura M.	1961	Asymmetry of Dst variations of geomagnetic storms with respect to he geomagnetic equator, Report UAG-R 122, Geophys. Inst. U. of Alaska, p. 12.
Sugiura M.	1964	Hourly values of the equatorial Dst for IGY in *Ann. Int. Geophys. Year*, Vol. 35, p. 945. Pergamon Press, Oxford.
Sugiura M. and Chapman S.	1960	The average morphology of geomagnetic storms with sudden commencement. Abhand. Akad. Wiss. Göttingen, Math. Physik Kl. Sonderh., Vol. 4.
Sugiura M. and Kamei T.	1991	Equatorial Dst index, IAGA Bulletin No. 40, ISGI Pub. Office, Saint-Maur-des-Fosses, France, June.
Sun W., Ahn B. H., Akasofu S. I. and Kamide Y.	1984	A comparison of the observed mid-latitude magnetic disturbance fields with those reproduced from the high latitude modeling current system. *J. geophys. Res.* **89,** 10881–10889.
Tarpley J. D.	1973	Seasonal movement of the Sq current foci and related effects in the equatorial electrojet. *J. atmos. terr. Phys.* **35,** 1063–1071.
Van Allen J. A.	1959	The geomagnetically trapped corpuscular radiation. *J. geophys. Res.* **64,** 1683–1689.
Van Allen J. A.	1969	Charged particles in the magnetosphere. *Rev. Geophys.* **7,** 233–255.
Vestine E. H., Laporte L., Lange I. and Scott W. E.	1947	The geomagnetic field; its description and analysis. Carnegie Inst. Wash. Pub. 580, 390 pp.
West B. J. and Shlesinger M.	1990	The noise in natural phenomena. *Amer. Sci.* **78,** 40–45.
Williams D. J.	1985	Dynamics of the Earth's ring current: theory and observations. *Space Sci. Rev.* **42,** 375–396.
Wrenn G. L.	1989	Persistance of the ring current 1958–1984. *Geophys. Res. Lett.* **16,** 891–894.